

Ultrafast charge carrier dynamics and photoelectrochemical properties of ZnO nanowires decorated with Au nanoparticles

Jason K. Cooper, Yichuan Ling, Yat Li*, Jin Z. Zhang*

Department of Chemistry and Biochemistry, University of California, Santa Cruz, CA 95064, USA.

*Corresponding author: Email: zhang@ucsc.edu, yli@chemistry.ucsc.edu

Phone: (831) 459-3776; Fax: (831) 459-2935

ABSTRACT

This study was designed to examine the possible photosensitization effect of zinc oxide (ZnO) nanowires (NWs) by Au nanoparticles (AuNPs) by directly monitoring the charge carrier lifetime in AuNP-decorated ZnO NWs. ZnO-Au nanocomposite structures showed reduced photocurrent compared to pristine ZnO NWs due to the combined effect of ZnO etching during the AuNPs growth and competitive absorption/scattering effects from AuNPs of incident UV photons. Ultrafast transient pump-probe spectroscopy was utilized to characterize the charge carrier dynamics. The bleach recovery of ZnO indicates electron-hole recombination on the 150 ps time scale attributed to shallow donor recombination. The AuNP-decorated ZnO NWs exhibit a fast decay of 3 ps in addition to the decays observed for ZnO NWs. This fast decay is similar to the hot electron relaxation lifetime observed for AuNPs in solution. Overall, the dynamics features for AuNP-decorated ZnO NWs appear as a simple sum of those from AuNPs and ZnO NWs alone. There is no evidence of photosensitization of the ZnO NWs by AuNPs investigated in this study.

Keywords: Au, ZnO, gold, nanowires, nanoparticles, dynamics, sensitization, transient absorption, PEC.

1 INTRODUCTION

Seeking renewable energy sources has driven interest in several research fields, one of which is in the use of metal oxide (MO) semiconductors for solar-driven water splitting.¹ The advances in nanoscience have resulted in tunable structural and electronic properties of MO materials to better suit the demands for photoelectrodes. One material of increasing interest is ZnO for several reasons including: wide-ranging options for shape control,² high electron mobility, abundance, non-toxic, and inexpensive cost. One dimensional (1D) ZnO nanowires are particularly interesting as they provide not only large surface area but also excellent vectorial charge carrier transport along nanowire growth axis.

While ZnO offer many benefits, it is a wide bandgap semiconductor (3.37 eV) which limits light absorption in the visible. There have been many studies aimed at extending the absorption range of such wide band-gap MOs into the visible including: sensitization with dyes,³ quantum dots,⁴⁻⁵ or doping.⁶ Another approach suggested recently has been the use of noble metal nanoparticles to extend the absorption range. By using the size- and shape-tunable surface plasmon resonance (SPR) of metal nanoparticles, it is possible to shift the absorption range of these structures from the UV to the near IR.⁷ An additional benefit to using noble metal nanoparticles could improve stability over organic dyes. A recent report showed that CdSe QD sensitized Au/TiO₂ hybrid films had improved PEC performance as compared to CdSe-TiO₂ while the Au/TiO₂ had reduced performance.⁸ The performance enhancement was attributed to increased light absorption from the CdSe due to scattering by the AuNPs. The performance reduction in the Au/TiO₂ system was found to be due to electron trapping from the Au. There have been other reports which have claimed sensitization effects by the Au *via* transference of photoexcited electrons to the conduction band (CB) of the MO.⁹⁻¹⁰ Other reports suggest that AuNPs facilitate charge separation by trapping excited electrons to minimize recombination in the MO.¹¹ These studies suggest that the effect of AuNPs is closely related to the coordination environment and the experimental

conditions. To better understand the role of AuNPs in the metal-semiconductor composite structure for water splitting, we managed to probe the excited state dynamics of the ZnO NWs both with and without decoration by AuNPs. The results will provide direct evidence for the role of AuNPs as a quencher or sensitizer. Carrier trapping would have the effect of shortening the ZnO lifetime while sensitization with AuNPs would inject electrons into ZnO and result in shorter hot electron lifetime in AuNPs or longer electron lifetime for ZnO.

We observed that the charge carrier dynamics of ZnO NWs and AuNPs act independently and no sensitization effects could be determined. From these results, AuNPs alone do not appear function as photosensitizers for ZnO.

2 EXPERIMENTAL SECTION

2.1 Synthesis

2.1.1 Synthesis of ZnO NW arrays

ZnO NWs were grown on a ZnO nanoparticle seeded FTO substrate (Hartford Glass Company Inc.) using a hydrothermal method reported previously.¹² 5 mM zinc acetate in ethanol was deposited drop-wise (2 drops) onto FTO substrate and air dried. This step was repeated five times following by annealing at 350 °C for 30 minutes. The zinc acetate deposition and annealing processes were carried out twice to ensure a uniform coating of ZnO nanocrystals on the FTO substrate. This substrate was placed into a Teflon-lined stainless steel autoclave, filled with 20 mL aqueous solution containing 0.05 M zinc nitrate and 0.05 M hexamethylenetetramine. The sealed autoclave was heated in an electric oven at 90 °C for 6 hours. A uniform white film was coated on the FTO substrate. It was rinsed with deionized water and air dried. Finally, the sample was annealed in air at 550 °C for 3 hours to increase the crystallinity of ZnO nanowires and improve their contact to the substrate.

2.1.2 Gold nanoparticle synthesis

Gold nanoparticles were grown on ZnO nanowire surfaces using a hydrothermal method reported previously.¹⁰ FTO substrate coated with ZnO nanowires was placed into a Teflon-lined stainless steel autoclave filled with 10 mL of 1 mM chloroauric acid (HAuCl₄) solution with a pH range of 7 and 8, adjusted by sodium citrate (Na₃C₆H₅O₇·3H₂O). The sealed autoclave was heated in an electric oven at 120 °C for 1 hour. Finally, Au-attached ZnO NW array films were rinsed with deionized water and air dried.

2.2 Instrumentation

2.2.1 UV-vis and photoluminescence spectroscopy

Absorption and photoluminescence (PL) spectra were collected at room temperature with a Hewlett Packard 8452A diode array UV-Visible spectrometer with a spectral resolution of 2 nm and a Jobin Yuon Horiba FluoroMax-3 fluorometer. Fluorescence measurements were collected at room temperature on the solid substrates at 45° from both the excitation and emission windows with the excitation wavelength 340±5nm.

2.2.2 Microscopy

Scanning electron microscopy (SEM) was conducted using a FEI Quanta 3D FEG Dualbeam microscope. Histograms were created by measuring a minimum of 100 structures of interest using the ImageJ software package.¹³

2.2.3 Femtosecond laser and transient absorption measurement

The details of TA laser system have been previously described.¹⁴ Briefly, <150 fs 1mJ pulses centered at 795 nm were split to a optical parametric amplifier (OPA) and sapphire crystal. Samples were excited with 360 nm and 450 nm light at

220 nJ/pulse perpendicular to the film surface. The white light continuum (WLC), ranging from 430-800 nm, interrogated the sample and was monitored by a CCD detector where 500 pulses were averaged for each data point. A forward and reverse scan was collected and averaged resulting in 1000 averages per data point. The delay stage allowed for generation of a 1000 ps delay with temporal resolution of 10 fs. The decay traces were verified to ensure a linear response with excitation power.

2.2.4 Fabrication of NW photoanodes and PEC measurement

NW arrays were fashioned into photoanodes by soldering a copper wire onto a bare portion of FTO substrate. The substrate was then sealed on all edges with epoxy resin except for a working area of *c.a.* 0.15 cm². All PEC measurements were carried out in a three-electrode electrochemical cell, with a coiled Pt wire as a counter electrode and an Ag/AgCl electrode as a reference. The electrolyte was a 0.5 M Na₂SO₄ aqueous solution with a pH of 7. Linear sweep voltammograms were measured by a CHI 660D electrochemical station under simulated sunlight with a 150 W xenon lamp (Newport 6255) coupled with an AM 1.5 global filter (Newport 81094). All measurements were conducted with front side illumination.

3 RESULTS AND DISCUSSION

3.1 Electron microscopy studies

SEM images show that the as-grown ZnO NWs are uniform and vertically aligned with length of 1800±300 nm, and a diameter of 75±22 nm (**Figure 1**), and with uniform thickness and hexagonal morphology. The AuNPs grown on ZnO NWs samples (ZnO-Au) appear to have a random distribution around the circumference of the wires. The AuNP average size was measured to be 22±3 nm and appeared as fully formed spheres with little deformation at the interface of the Au and ZnO. The average ZnO NW diameter in this sample is slightly shrunk to 60±20 nm due to the Au formation reaction with the HAuCl₄ solution. Additionally, the wire morphology became conically shaped which is indicative of etching.

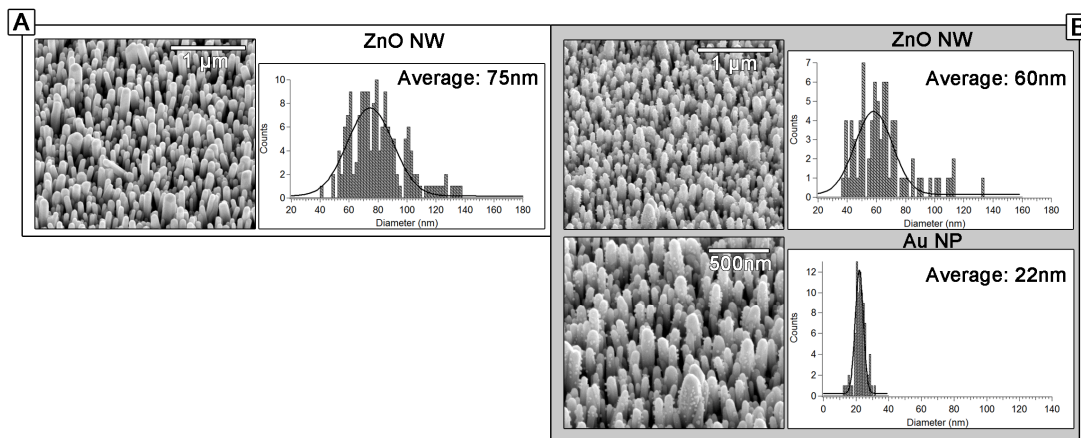


Figure 1. SEM images and histograms of the two samples studied A) ZnO, B) ZnO-Au.

3.2 Optical Spectroscopy

3.2.1 UV-Vis

The UV-Vis spectra of the two samples studied had very similar characteristics dominated by absorption and scattering, as shown in **Figure 2**. While band-edge absorption for ZnO with a bandgap of 3.37eV was expected to occur about 370 nm, this feature is overwhelmed by the large amount of scattering due to the large physical features of the sample. The monotonic increase in intensity towards shorter wavelength is consistent with Rayleigh scattering. The spectrum of the ZnO-Au sample has a distinguishable shoulder at 527 nm, attributed to SPR of the AuNPs, and increased absorbance across the entire wavelength range by a factor of about 1.6, likely due to increased light absorption and scattering from the AuNPs. Images of the two samples are shown in the inset of **Figure 2**.

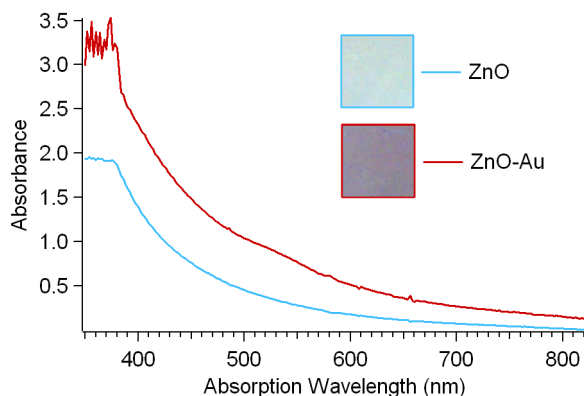


Figure 2: UV-Vis spectrum and digital images of ZnO (blue) and ZnO-Au (red).

3.2.2 Photoluminescence

The PL spectra of the two samples studied are shown in **Figure 3A** and **3B** presented “as-collected” and normalized to the maximum, respectively. The most notable feature is the near band-edge emission between 370-390 nm for the samples. The peak is at 387 nm (3.20 eV) for ZnO and 385 nm (3.22 eV) for ZnO-Au. These features have been attributed to donor recombination in ZnO.¹⁵ The ZnO and ZnO-Au samples had essentially identical spectra, upon normalization, with the exception of a dip in intensity centered about 524 nm which is attributed to re-absorption by the AuNPs. Due to the difference in absorption/scattering between the samples, we attribute the decreased emission in the ZnO-Au to re-absorption and increased scattering by AuNPs over the UV region as well. This assignment is supported by observations made in the transient absorption studies to be discussed later. In addition, both samples show some green emission centered at 550 nm which has been previously described due to neutral oxygen vacancies (V_O);¹⁶ however, this feature had a very low intensity as compared to the bluer feature.

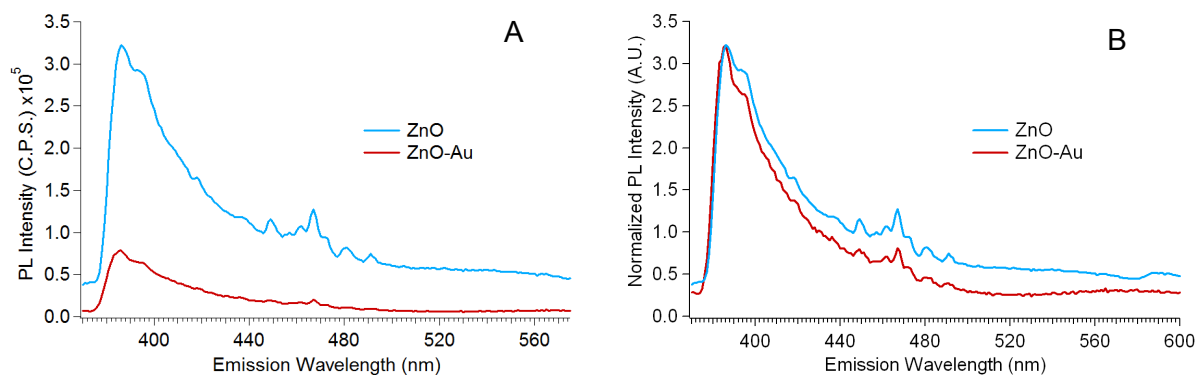


Figure 3: A) Fluorescence spectrum taken at 23°C of ZnO (blue) and ZnO-Au (red), “as-collected.” B) Normalized fluorescence spectrum of the same samples. Excitation wavelength: 340nm.

3.3 Photoelectrochemical Water Splitting

The linear sweep voltammograms for the pristine ZnO NW arrays and ZnO decorated with AuNPs are illustrated in **Figure 4**. In comparison to pristine ZnO, ZnO-Au show a dramatic decrease in photocurrent density at applied potentials above 0.6 V vs. RHE. Based on the morphology change observed by SEM, the reduced photocurrent for the ZnO-Au sample could be attributed to decreased available UV photons for absorption by ZnO due to the surface-attached AuNPs as well as the reduced volume of ZnO NWs due to the etching effect of acidic H₂AuCl₄. The reduced photocurrent in this type of system as observed in this work is consistent with our previous studies.⁸

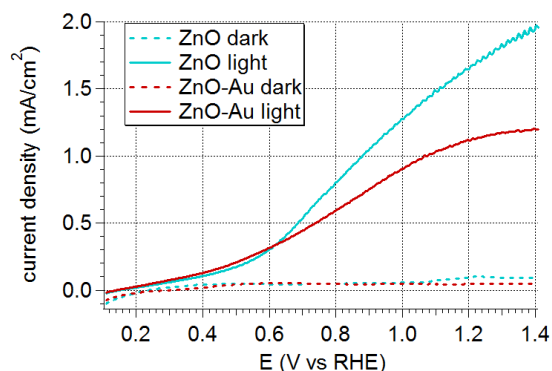


Figure 4: Linear sweep voltammograms collected for ZnO (blue) and ZnO-Au (red) in 0.5 M Na₂SO₄ electrolyte (pH = 7) under simulated sunlight illumination at 100 mW/cm². Dark scans are also reported with the same coloring but dashed lines.

3.4 Transient Absorption Spectroscopy

In an effort to understand the electron dynamics in the ZnO-AuNP composite and if AuNPs can sensitize ZnO, we used transient absorption (TA) pump probe spectroscopy to determine the excited state lifetimes of the composite and constituent materials. The TA system is equipped with a tunable pump source and white light probe (420-800 nm) making it is possible to excite the AuNP only (450 nm) or to excite both materials at the same time (360 nm).

The transient time profiles for the different samples and two excitation wavelengths are shown as contour plots in **Figure 5**. The TA signals with intensity indicated by color are plotted as a function of probe wavelength and delay time between the pump and probe pulses. The pump wavelengths used are indicated at the top of each row (450 nm and 360 nm).

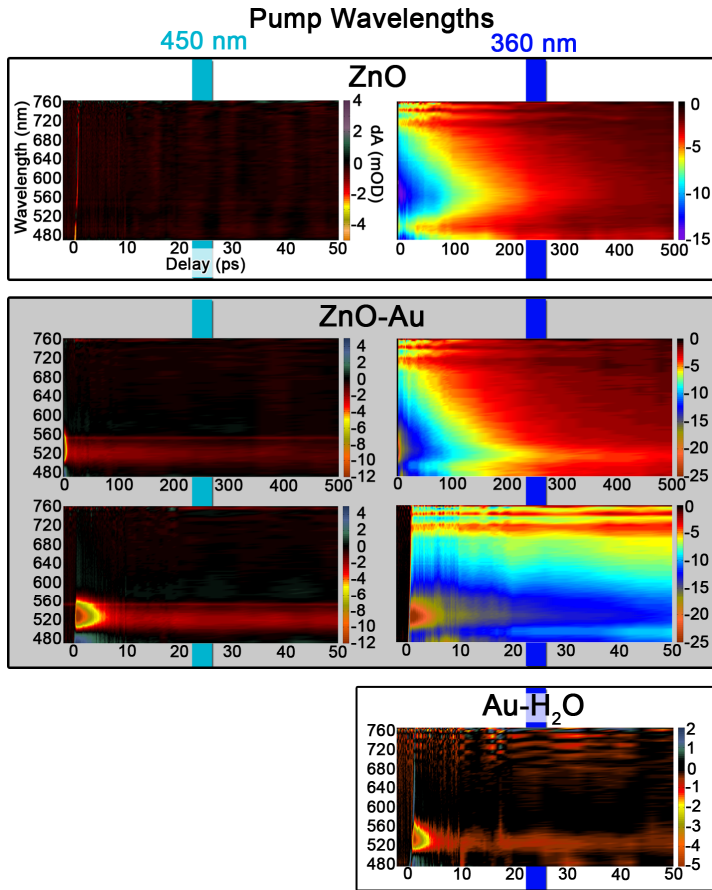


Figure 5. Contour plots of TA data of ZnO (top-white background), ZnO-Au (middle-gray background), and AuNP in H₂O (bottom-white background) over the 50 and 500ps delay ranges as pumped with 450nm (turquoise line) and 360nm (blue line). Each plot is of wavelength (nm), delay (ps), and TA (mOD) color as reported on the right of each figure; see top left figure for units.

As a control experiment, the decant from the synthesis of the ZnO-Au sample was collected which contained a suspension of only the AuNPs in water. This sample, when excited with 360 nm pump (**Figure 5**, bottom right), displays a very fast component with a time constant of 2.3 ± 0.4 ps and a small amplitude slow decay component with a lifetime of 360 ± 70 ps. The feature is Gaussian shaped and centered at around 525 nm which is strictly due to the SPR from AuNPs. The fast component is due to electron-phonon coupling and the slower decay is due to phonon relaxation.¹⁷

The TA spectrum of ZnO following 360 nm excitation (**Figure 5**, top right) has its highest intensity toward the blue and tails to lower intensity toward the red. This transient bleach feature mostly decays within 250 ps however a longer lived component was observed extending through the 500 ps time window. Under 450 nm excitation, the signal is entirely absent indicating that the transient bleach observed with the 360 nm pump is due to excitons. For a typical sample, a bleach signal indicates reduced ground state absorption under pumped perturbation. While ZnO does not absorb over our white light range, it is important to note that optical density is the sum of both absorption and scattering. Inspection of the UV-Vis spectrum in **Figure 1** indicates that the ZnO NW sample scatters strongly. The origin of the bleach signal would therefore imply that there was less scattering under pump pulse excitation, which would result in more probe light reaching the detector, making the differential absorption negative. In order for less scattering to occur, the refractive index of the material would have increased while electrons were in the excited state following photoexcitation. The excited state electrons effectively increase the permittivity of the material thereby increasing the refractive index.¹⁸ While increased permittivity under UV-illumination of ZnO nanowires has been reported¹⁹, it has not yet been used to

characterize the lifetime of the material with this method, to the best of our knowledge. The monotonic increase in intensity towards shorter wavelengths, as observed in **Figure 5**, supports this assignment.

The ZnO-Au sample under 450 nm pump (**Figure 5**, middle panel top left) has a very weak longer lived component centered around 525 nm, as can be observed in the 500 ps time window, with a much faster and intense feature which is only seen at the very beginning of the TA spectrum. The expanded time domain of this spectrum, shows that this feature is very fast (3-4ps) and is Gaussian-shaped centered around 525 nm. The same feature can be seen in the 360 nm pump data. The longer component appears in the 500 ps time window centered around 525 nm as a pointed streak feature on-top of a feature that mirrors the ZnO signal. There is a fast component observed in the 50 ps window which has the same features as those observed in the 450 nm pump plot. We attribute the fastest Gaussian feature to the AuNP electron-phonon coupling.

The ZnO-Au sample under 450 nm pump, therefore, has transient bleach signal from the AuNPs only. As a result it is clear that they do not result in any signal that can be attributed to electron injection into the CB of ZnO. In addition, while both materials are excited in the ZnO-Au sample with the 360 nm pump, there does not appear to be any changes in the transient decay profiles as compared to the ZnO sample alone. These results also suggest that excited electrons in the ZnO are not affected by the AuNPs, as the ZnO sample was expected to have a shortened lifetime if the excited electrons could decay through a AuNP pathway or AuNP induced trap states.

To make it easier to obtain time constants of the lifetimes, we plotted the TA signal as a function of time for a particular probe wavelength. For example, the TA signal with the 524 nm probe wavelength is shown in **Figure 6**. This particular wavelength was selected as it illustrates the maximum bleach signal for the Au yet also contains the bleach recovery signal for the ZnO. All the samples characterized have pulse width limited rise times. The AuNPs alone in H₂O, shown in a 50 ps window only, have a very fast initial decay with an incomplete return to baseline. Examination of the ZnO decay plot shows a single exponential bleach recovery which has a small amplitude longer component that manifests as an incomplete return to baseline within the examined time window. The ZnO-Au under 450 nm pump has a very fast initial decay which also has an additional component which is slow to return to baseline. The same sample under 360 nm excitation appears as the sum of the ZnO-Au (450 nm) and the ZnO (360 nm) decays with a very fast component which decays to a single exponential followed by an additional low amplitude component which is much slower. Furthermore, the full time window (**Figure 6**, left panel) shows the ZnO and ZnO-Au bleach recoveries are identical. This would not be expected if the ZnO electrons could decay through AuNP pathways which would shorten the ZnO lifetime. This indicates that there is a lack of interaction or charge transfer between the two materials; as a result, the charge carriers in both act independently from one another.

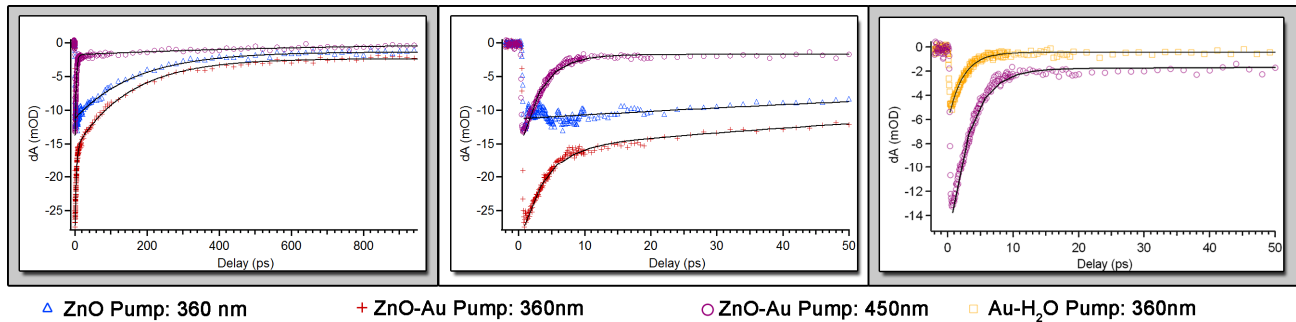


Figure 6: Transient bleach recovery traces of the 524 nm probe of ZnO pump 360 nm (blue triangle), ZnO-Au pump 360 nm (red cross), ZnO-Au pump 450 nm (purple circle), Au in water (Au-H₂O) pump 360 nm (yellow square).

To better understand the lifetime of these components, the decay traces were fit with single or double exponentials with an offset to account for the slowest unresolved component. The fit results are shown as black lines in **Figure 6** and the

time constants and amplitudes are reported in **Table 1**. The fit results show that under 360 nm pump the Au-H₂O could be fit with a double exponential with a time constant of 2.3±0.4 ps and 360±70 ps, the ZnO sample could be fit with a single exponential with time a time constant of 160±20 ps, the ZnO-Au was fit with a double exponential with time constants of 3.5±0.5 ps and 150±20 ps. The ZnO-Au pumped with 450 nm was fit with a single exponential with time constant of 3.2±0.5 ps.

Table 1: Fitting results of the ZnO, ZnO-Au, and Au-H₂O 524 nm probe showing the pump wavelength, amplitude (A), and lifetime (τ).

Sample	Pump (nm)	Probe (nm)	A₁	τ_1 (ps)	A₂	τ_2 (ps)
ZnO	360	524			-10	160 (20)
	450	524				
ZnO-Au	360	524	-15	3.5 (0.5)	-13	150 (20)
	450	524	-15	3.2 (0.5)		
Au-H ₂ O	360	524	-8	2.3 (0.4)	-6	360 (70)

The ZnO components are consistent with other observations, however assignments of these components are varied.²⁰⁻²² Charge carrier cooling is reported to be <200 fs²³ and typical observations of the electron-hole plasma (EHP) are within the first few ps,^{20, 24-25} while green trap state emission due to V_O is reported in the μ s range.^{16, 26-27} Radiative recombination has been reported to be single exponential with a lifetime of 259 ps at 2K from the Γ_5 free excitons.²⁸ As the pump power used in this experiment was low and generated a linear relationship between power and signal intensity, we attribute the observed component to shallow donor bound exciton recombination. This recombination lifetime was identical between the ZnO and ZnO-Au sample, considering error. Therefore, the addition of AuNPs on the surface of the NWs did not affect the ZnO lifetime by introducing trap states or charge transfer mechanisms to the exciton recombination.

The hot electron lifetime of the AuNPs on the ZnO NWs under 360 and 450 nm are identical within the error of measurement. However, it is slightly longer for the ZnO-Au sample than was the AuNPs in water, 3.2±0.5ps vs. 2.3±0.4ps. This is likely due to the difference in the dielectric constant between ZnO/air and water. These results confirm the assertion that the reduced photocurrent seen in the ZnO-Au sample is not due to electron trapping by the AuNPs but rather due to competitive absorption and increased back scattering of UV photons by the AuNPs.

4 CONCLUSION

We have characterized pristine ZnO NWs and ZnO NWs decorated with AuNPs with the intention of understand if AuNP could act as a sensitizer for the ZnO in the visible. From the increased absorption in the UV-Vis spectra we concluded that the AuNPs increase the scattering and absorption. The PL spectra showed reduced emission with the AuNPs which we attributed to re-absorption and scattering. The PEC data showed decreased photocurrent in the AuNP-decorated ZnO NW sample as compared to pristine ZnO NWs. Time dependent bleach recovery the ZnO-Au sample under 360 nm excitation is essentially a simple sum of the results of the ZnO-Au and ZnO samples. The fitting results confirmed there was no effect on the lifetime of ZnO NWs due to the presence of AuNPs and visa versa. We therefore conclude that the reduced PEC performance in the ZnO-Au sample was due to increased scattering/absorption of charge carrier generating photons by the AuNPs. The results therefore do not provide any indication that AuNPs sensitize ZnO under the conditions used in our study. Further research is clearly needed to determine if photosensitization of MO with metal nanoparticles if possible and, if yes, what the necessary conditions are.

5 ACKNOWLEDGEMENTS

Special thanks to Damon Wheeler and Rebecca Newhouse for their technical support. JZZ acknowledges support by the Basic Energy Science Division of the US DOE (DE-FG02_ER46232) and by the US NSF. Y.L. acknowledges the financial support of this work in part by NSF (DMR-0847786).

6 REFERENCES

- [1] Yang, X., Wolcott, A., Wang, G., Sobo, A., Fitzmorris, R. C., Qian, F., Zhang, J. Z.; Li, Y., "Nitrogen-doped ZnO nanowire arrays for photoelectrochemical water splitting," *Nano Lett.* 9(6), 2331-2336 (2009).
- [2] Wang, Z. L., "Nanostructures of zinc oxide," *Materials Today* 7(6), 26-33 (2004).
- [3] Law, M., Greene, L. E., Johnson, J. C., Saykally, R.; Yang, P., "Nanowire dye-sensitized solar cells," *Nat. Mater.* 4(6), 455-459 (2005).
- [4] Leschkies, K. S., Divakar, R., Basu, J., Enache-Pommer, E., Boercker, J. E., Carter, C. B., Kortshagen, U. R., Norris, D. J.; Aydil, E. S., "Photosensitization of ZnO nanowires with CdSe quantum dots for photovoltaic devices," *Nano Lett.* 7(6), 1793-1798 (2007).
- [5] Wang, G., Yang, X., Qian, F., Zhang, J. Z.; Li, Y., "Double-sided CdS and CdSe quantum dot co-sensitized ZnO nanowire arrays for photoelectrochemical hydrogen generation," *Nano Lett.* 10(3), 1088-1092 (2010).
- [6] Ahn, K. S., Yan, Y., Shet, S., Deutsch, T., Turner, J.; Al-Jassim, M., "Enhanced photoelectrochemical responses of ZnO films through Ga and N codoping," *Appl. Phys. Lett.* 91, 231909 (2007).
- [7] Preciado-Flores, S., Wang, D., Wheeler, D. A., Newhouse, R., Hensel, J. K., Schwartzberg, A., Wang, L., Zhu, J., Barboza-Flores, M.; Zhang, J. Z., "Highly reproducible synthesis of hollow gold nanospheres with near infrared surface plasmon absorption using PVP as stabilizing agent," *J. Mater. Chem.*, (2010).
- [8] Liu, L., Wang, G., Li, Y.; Zhang, J. Z., "CdSe quantum dot-sensitized Au/TiO₂ hybrid mesoporous films and their enhanced photoelectrochemical performance," *Nano Research* 4(3), 249-258 (2011).
- [9] Du, L., Furube, A., Yamamoto, K., Hara, K., Katoh, R.; Tachiya, M., "Plasmon-Induced Charge Separation and Recombination Dynamics in Gold- TiO₂ Nanoparticle Systems: Dependence on TiO₂ Particle Size," *J. Phys. Chem. C* 113(16), 6454-6462 (2009).
- [10] Chen, Z. H., Tang, Y. B., Liu, C. P., Leung, Y. H., Yuan, G. D., Chen, L. M., Wang, Y. Q., Bello, I., Zapien, J. A., Zhang, W. J., Lee, C. S.; Lee, S. T., "Vertically Aligned ZnO Nanorod Arrays Sensitized with Gold Nanoparticles for Schottky Barrier Photovoltaic Cells," *J. Phys. Chem. C* 113(30), 13433-13437 (2009).
- [11] Dawson, A.; Kamat, P. V., "Semiconductor-metal nanocomposites. photoinduced fusion and photocatalysis of gold-capped TiO₂ (TiO₂/gold) nanoparticles," *The Journal of Physical Chemistry B* 105(5), 960-966 (2001).
- [12] Greene, L. E., Law, M., Goldberger, J., Kim, F., Johnson, J. C., Zhang, Y., Saykally, R. J.; Yang, P., "Low Temperature Wafer Scale Production of ZnO Nanowire Arrays," *Angewandte Chemie International Edition* 42(26), 3031-3034 (2003).
- [13] Abramoff, M. D., Magalhaes, P. J.; Ram, S. J., "Image Processing with ImageJ," *Biophotonics International* 11(7), 36-42 (2004).
- [14] Newhouse, R. J., Wang, H., Hensel, J. K., Wheeler, D. A., Zou, S.; Zhang, J. Z., "Coherent Vibrational Oscillations of Hollow Gold Nanospheres," *J. Phys. Chem. Lett.* 2(3), 228-235 (2011).
- [15] Meyer, B., Alves, H., Hofmann, D., Kriegseis, W., Forster, D., Bertram, F., Christen, J., Hoffmann, A., Straßburg, M.; Dworzak, M., "Bound exciton and donor-acceptor pair recombinations in ZnO," *physica status solidi (b)* 241(2), 231-260 (2004).
- [16] De Angelis, F.; Armelao, L., "Optical properties of ZnO nanostructures: a hybrid DFT/TDDFT investigation," *Phys. Chem. Chem. Phys.* 13, 467-475 (2011).
- [17] Hartland, G. V., "Measurements of the material properties of metal nanoparticles by time-resolved spectroscopy," *Phys. Chem. Chem. Phys.* 6(23), 5263-5274 (2004).
- [18] Katkar, R. A., Ramanathan, S., Bandyopadhyay, S.; Tait, G., "Wire-size-dependent optical activity in electrochemically self-assembled II-VI semiconductor nanowire arrays," *Physica E: Low-dimensional Systems and Nanostructures* 40(3), 556-560 (2008).

- [19] Katkar, R. A.; Tait, G. B., "The effect of stationary ultraviolet excitation on the optical properties of electrochemically self-assembled semiconductor nanowires," *J. Appl. Phys.* 101(5), 053508-053508-7 (2007).
- [20] Yamamoto, A., Kido, T., Goto, T., Chen, Y., Yao, T.; Kasuya, A., "Dynamics of photoexcited carriers in ZnO epitaxial thin films," *Appl. Phys. Lett.* 75, 469 (1999).
- [21] Mehl, B. P., Kirschbrown, J. R., House, R. L.; Papanikolas, J. M., "The End is Different than the Middle: Spatially Dependent Dynamics in ZnO Rods Observed by Femtosecond Pump-Probe Microscopy," *J. Phys. Chem. Lett.* 2, 1777-1781 (2011).
- [22] House, R. L., Mehl, B. P., Kirschbrown, J. R., Barnes, S. C.; Papanikolas, J. M., "Characterizing the Ultrafast Charge Carrier Trapping Dynamics in Single ZnO Rods Using Two-Photon Emission Microscopy," *J. Phys. Chem. C* 115, 10806-10816 (2011).
- [23] Sun, C. K., Sun, S. Z., Lin, K. H., Zhang, K. Y. J., Liu, H. L., Liu, S. C.; Wu, J. J., "Ultrafast carrier dynamics in ZnO nanorods," *Appl. Phys. Lett.* 87, 023106 (2005).
- [24] Kwok, W., Djurišić, A., Leung, Y., Chan, W.; Phillips, D., "Time-resolved photoluminescence from ZnO nanostructures," *Appl. Phys. Lett.* 87, 223111 (2005).
- [25] Hendry, E., Koeberg, M.; Bonn, M., "Exciton and electron-hole plasma formation dynamics in ZnO," *Physical Review B* 76(4), 045214 (2007).
- [26] Zhang, S., Wei, S. H.; Zunger, A., "Intrinsic n-type versus p-type doping asymmetry and the defect physics of ZnO," *Physical Review B* 63(7), 075205 (2001).
- [27] Lany, S.; Zunger, A., "Anion vacancies as a source of persistent photoconductivity in II-VI and chalcopyrite semiconductors," *Physical Review B* 72(3), 035215 (2005).
- [28] Reynolds, D., Look, D., Jogai, B., Hoelscher, J., Sherriff, R., Harris, M.; Callahan, M., "Time-resolved photoluminescence lifetime measurements of the and free excitons in ZnO," *J. Appl. Phys.* 88, 2152 (2000).